Analysis of Intraplate Earthquakes and Deformation in the Indo-Australian Plate: Moment Tensor and Focal Depth Modeling

Honor's Thesis
by
Wardah Mohammad Fadil

Department of Earth and Environmental Sciences
University of Michigan

Abstract

The April 2012 sequence of $M_W > 8.0$ strike-slip earthquakes off the northern coast of Sumatra and the May 2014 ~50 km deep earthquake in the Bay of Bengal are rare intraplate earthquakes that have sparked numerous studies on internal deformation of the Indo-Australian Plate. In this thesis, we conducted moment tensor analysis and observed the NW/SE pattern of compression in the southern Indian Ocean, perpendicular to the compression directions at the Sunda Trench. We estimated principal stress directions for a cluster of 55 intraplate earthquakes in the southern Indian Ocean, demonstrating that they are consistent with the general stress directions in the region. Analysis of depth phase arrival times and surface wave dispersion for the May 21 2014 Bay of Bengal earthquake at the BJT and PALK seismic stations confirmed the 40-60 km focal depth of the earthquake. The occurrence of intraplate earthquakes and orientation of stress within the Indo-Australian Plate indicate the complex and dynamic plate boundary forces and the formation of a diffuse deformation zone. However, the causes of deep focal depths of intraplate earthquakes are still ambiguous.

1. Introduction

The Indo-Australian Plate is a unique tectonic plate. It includes the continents of India and Australia and the surrounding oceanic lithosphere. The plate formed approximately 42 million years ago when the Indian and Australian plates fused together [Royer et al, 1991; Cande and Kent, 1995; Krishna et al, 1995]. The plate boundaries are characterized by mid-ocean ridge spreading, and ocean-continent and continent-continent collisions. The Carlsberg Ridge and Central Indian Ridge separate the African plate from the Indo-Australian Plate while the Southeast Indian Ridge separates the Antarctic Plate from the Indo-Australian Plate. The Central Indian Ridge, Southeast Indian Ridge and Southwest Indian Ridge meet at the Rodrigues Triple Junction. In the east, the Indo-Australian Plate is subducting beneath the Sunda plate at the

Sunda Trench while the Pacific Plate is subducting under the Indo-Australian Plate at the Tonga-Kermadec Trench. In the north, the collision of the Indian continent with Eurasia has produced continuing uplift of the Himalayas.

Internal deformation and stresses are strong within the Indo-Australian Plate. This is evident from the relatively large number of moderate-size intraplate earthquakes. The Global CMT catalog [Dziewonski et al, 1981; Ekstrom et al, 2012] includes more than 36,000 earthquakes with $M_W > 5$ that occurred globally from January 1980 to April 2016. This is the highest intraplate seismicity among all plates. The concentration of intraplate earthquakes in the southern Indian Ocean (Fig. 1) may be associated with the formation of a diffuse deformation zone and eventual break-up of the Indo-Australian Plate into four subplates; the Indian Plate, Capricorn Plate, Australian Plate and Macquarie Plate [DeMets et al, 2009]. In addition to high intraplate seismicity, the diffuse deformation zone is characterized by the predominantly north-south oriented compressive stress near the Ninety East Ridge and Wharton Basin [Cloetingh and Wortel, 1986; Muller et al, 2014]. The convergence of the Indo-Australian Plate with the Eurasian plate at a slower rate of ~40 mm/year compared to the subduction rate of ~70 mm/year at the Sunda Trench [Whittaker et al, 2007] may cause the high compressive stress within the plate.

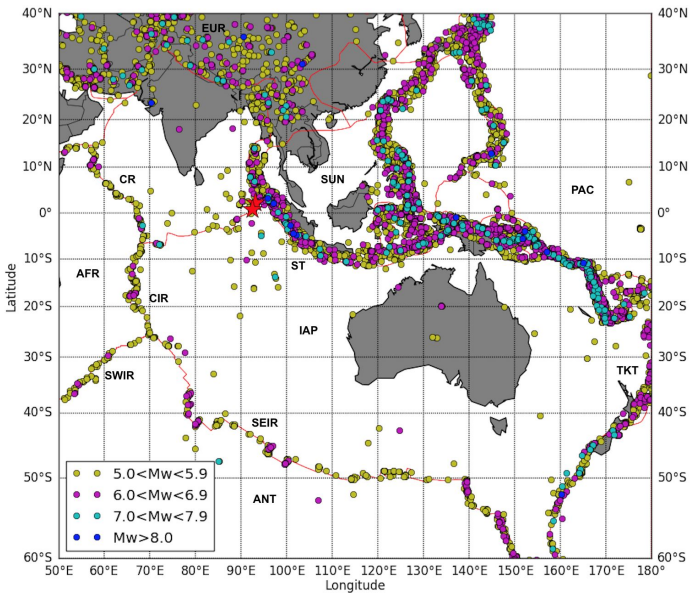

Fig 1. Map of earthquakes with $M_W > 5.0$ in the Indo-Australian Plate from January 1980 - April 2016. The April 2012 M_W8.7 and M_W8.2 intraplate strike slip earthquakes are plotted as red stars. Abbreviations are as follows: IAP, Indo-Australian Plate; ANT, Antarctic Plate; AFR, African Plate; EUR, Eurasian Plate; SUN, Sunda Plate; PAC, Pacific Plate; CR, Carlsberg Ridge; CIR, Central Indian Ridge; SEIR, Southeast Indian Ridge; SWIR, Southwest Indian Ridge; ST, Sunda Trench; TKT, Tonga-Kermadec Trench.

The April 11 2012 M_W 8.7 and M_W 8.2 strike-slip intraplate earthquakes are the largest recorded strike-slip intraplate earthquakes within the Indo-Australian Plate (Fig 1). The earthquakes occurred 100−200 km seaward of the Sumatra subduction zone and were followed by numerous aftershocks between M_W 5.0−7.0. Yue et al, [2012] associated the earthquake sequence with the India-Eurasia continental collision and slab pull in the Sumatra subduction zone and argued that the strike-slip faulting involved the rupture of a complex network of pre-existing fracture zones in the oceanic lithosphere. Satriano et al [2012], and Andrade et al [2014] related the April 2012 earthquake sequence to the reactivation of faults along the Ninety East Ridge and Wharton Basin.

Fig 1 shows a magnitude plot and Fig 2 shows a source depth plot of $M_W > 5$ earthquakes that have occurred in the Indo-Australian Plate since Jan 1980. The earthquakes that occur on the convergent boundary of the Indo-Australian Plate range from $5.0 < M_W < 10.0$ and most of the larger magnitude earthquakes concentrate along this boundary as seen along the Himalayan Front, Sunda Trench, Java Trench and Tonga Trench. Earthquakes at the extensional boundary are mostly between $5.0 < M_W < 7.0$. Most intraplate earthquakes have magnitudes lower than M_W 6.0. However, several $M_W > 6.0$ events have occurred in the equatorial Indian Ocean; near the Central Indian Ridge, and within the Ninetyeast Ridge and Wharton Basin.

As expected, many subduction zone earthquakes on the Indo-Australian Plate interface are deeper than 15 km (Fig 2). At the extensional boundaries, as seen at the Carlsberg Ridge, Central Indian Ridge and Southeast Indian Ridge, the depth of the earthquakes range from crustal source depths to upper mantle source depths and are dominated by earthquakes with depths between 15-20 km. At the Sunda Trench and Tonga-Kermadec Trench, the earthquake depths also range widely from crustal source depths to upper mantle source depths. Shallow earthquakes at subduction zones are associated with outer-rise earthquakes while the deep earthquakes are associated with the deformation of the subducting slab. The earthquake source depths at the Himalayan Front also range from crustal source depths to upper mantle source depths. Most intraplate earthquakes are shallow. However, according to the Global CMT catalog, several intraplate earthquakes with strike-slip mechanisms were deeper than 50 km. These include a M_W 6.1 earthquake in the Bay of Bengal on 21 May 2014 at a depth of 57.6 km and the M_W 8.2-8.6 sequence off the west coast of Northern Sumatra on 11 April 2012 between depths 45 km and 55 km. Oceanic intraplate earthquakes with hypocenters deeper than 15 km are considered unusual since they occur in the upper mantle or deeper in the Earth. We expect deep earthquakes to occur in a subduction zone tectonic setting and intraplate earthquakes to be limited to depths above the upper mantle.

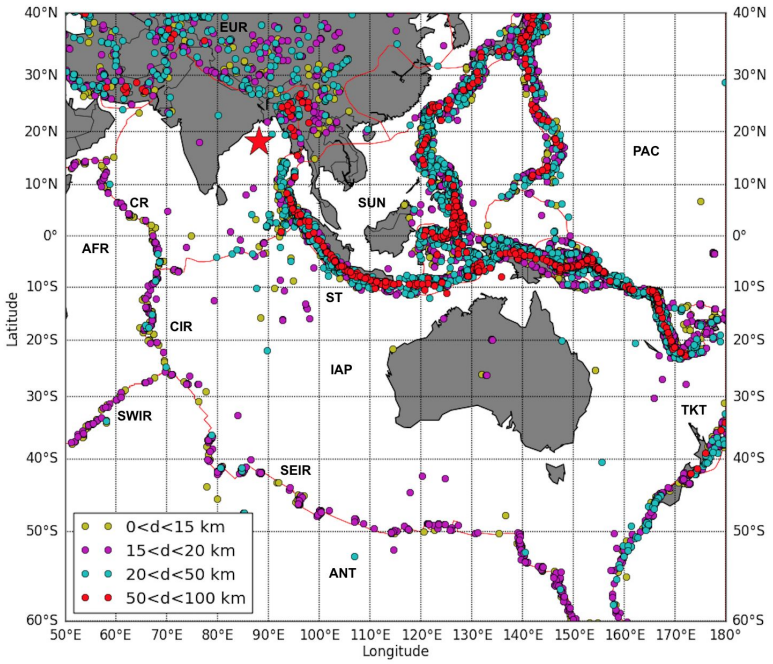

Fig 2. Map of earthquake source depths for earthquakes with Mw>5.0 in the Indo-Australian Plate from January 1980 - April 2016. The May 21 2014 Bay of Bengal earthquake is plotted as a red star. Abbreviations are as follows: IAP, Indo-Australian Plate; ANT, Antarctic Plate; AFR, African Plate; EUR, Eurasian Plate; SUN, Sunda Plate; PAC, Pacific Plate; CR, Carlsberg Ridge; CIR, Central Indian Ridge; SEIR, Southeast Indian Ridge; SWIR, Southwest Indian Ridge; ST, Sunda Trench; TKT, Tonga-Kermadec Trench.

The May 21 2014 M_W 6.1 Bay of Bengal earthquake occurred ~300 km off the east coast of India in a relatively low seismicity region. It is isolated from other clusters of moderate intraplate earthquakes and only 7 earthquakes of $5<M_W<5.5$ have occurred within a radius of 400 km of its epicenter, since 1970. It was followed by three $M_W < 6$ aftershocks, all of which occurred within 50 km of the epicenter [Mallick and Rajendran, 2015]. The focal mechanism reported by Global CMT indicates that it was a strike-slip event that occurred along steeply dipping NW-SE or NE-SW fault planes. The focal depth, fault orientation and causes of this earthquake has been actively researched and discussed but the results are still ambiguous. Research on this earthquake has been limited to digital waveform analysis due to the fact that the crust is overlain by ~12 km thick sediments from the Bengal Fan and very little seismogenic structures in the area have been mapped [Rao et al, 2015]. In this thesis, I will conduct waveform analysis and further discuss other research findings on this earthquake.

This thesis is focused on intraplate seismicity in the northwest Indo-Australian plate, covering the Central Indian Basin, Ninetyeast Ridge, Wharton Basin and Bay of Bengal. In this thesis, I use the Global CMT (gCMT) catalog to study the orientation of the principal stress axes of intraplate earthquakes in the Indo-Australian Plate (Section 2). In Section 3, I estimate by linear least squares regression of slip directions, a deviatoric stress tensor for a region in the

southern Indian Ocean using the largest cluster of intraplate earthquakes. In Section 4, I analyze the waveforms of the May 2014 Bay of Bengal earthquake to verify the unusually large source depths reported in the catalog. In Section 5, I discuss the main findings of my thesis work.

2. Analysis of the moment tensors: principal axes

2.1 P-axis Directions

The seismic moment tensor is the most general description of the earthquake source mechanism. It is a symmetric 3×3 tensor that represents the equivalent force-couples of the earthquake. After rotation of the reference frame, the diagonal of the moment tensor include the strengths of the three orthogonal principal stress axes; the directions of maximum compressive stress (P-axis), minimum compressive stress (T-axis) and null axis (N-axis). The best double-couple component of the moment tensor is equivalent to the focal mechanism (popularly known as the 'beachball diagram'), that indicates the average direction of slip and the orientation of the fault. Two orthogonal nodal planes separate the four compressional (or P) and dilatational (or T) quadrants. The P-axis and the T-axis indicate the maximum compressional and extensional stresses and correspond to the directions of highest amplitude P wave radiation. We focus on the orientation of the P-axis of all intraplate earthquakes in the Indo-Australian Plate. We visualize the state of stress within the plate by plotting the P-axis directions of these earthquakes. Only earthquakes with horizontal P-axis, plunging less than 20°, are plotted to identify the pattern of horizontal compression within the plate and its relation to the plate motions and regional stress fields.

2.2 Results

Throughout the Indo-Australian Plate, the P-axes of intraplate earthquakes rotate from NE-SW in the southeast towards NW-SE in the northwest and NE-SW in the Bay of Bengal (Fig. 3). On average, the P-axis of intraplate earthquakes in the diffuse deformation zone comprising of the Central Indian Basin, Ninety East Ridge and Wharton Basin and the M_W 8.7 and M_W 8.2 strike-slip earthquakes in April 2012, are oriented predominantly NW-SE. This is roughly perpendicular to the P-axis direction of the subduction zone earthquakes along the Sunda Trench and the plate motion direction. The P-axis directions of earthquakes along the Himalayan Front reflect the NE-SW collision of India with Eurasia. Along the spreading ridges, the P-axis directions are mostly parallel to or make a 45° angle with the spreading ridge due to ridge spreading and transform faulting, respectively.

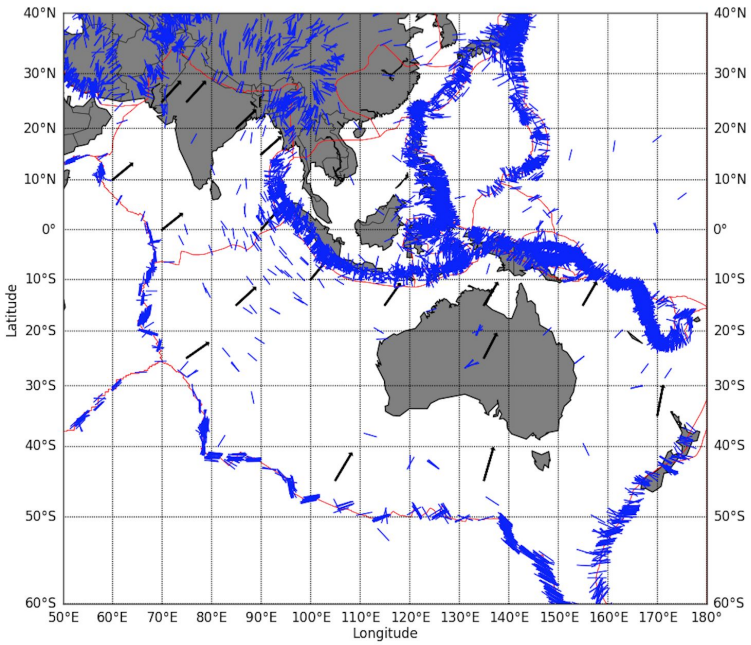

Fig 3. Map of earthquake P-axis directions in the Indo-Australian Plate for earthquakes that occurred from January 1980 - April 2016. Black arrows indicate relative plate motion [Plate Motion Calculator].

3. Analysis of the moment tensors: deviatoric stress in the Indian Ocean

3.1 Inversion of slip directions

To quantify the state of stress within the Indo-Australian Plate, we determine the deviatoric stress tensor based on 55 intraplate earthquakes with $M_W > 5.0$ near the Ninetyeast Ridge and in the Wharton Basin region (Fig 4). By linear least-squares inversion of slip directions we estimate the deviatoric stress tensor that represents the state of stress within the region. We use the methods of Michael [1984] which are valid under the assumption that the earthquakes are independent and represent the same stress tensor and that the tangential traction on the fault planes are similar and parallel to the slip direction:

$$\hat{t} = \frac{\vec{\tau}(\hat{n}, \sigma)}{|\vec{\tau}(\hat{n}, \sigma)|} = \hat{s}$$

where $\vec{\tau}(\hat{n}, \sigma)$ is the tangential traction on the fault plane with unit normal $\hat{n}$, due to the deviatoric stress tensor σ and $\hat{\tau}$ is the unit vector associated with $\vec{\tau}$. The tangential traction on the fault plane is equivalent to

$$\vec{\tau} = \sigma\hat{n} - [(\sigma\hat{n}) \cdot \hat{n}]\hat{n}$$

where $\bar{\tau}$ is linear with respect to σ, however, $|\bar{\tau}|$ is not. To linearize the inversion for σ, we assume that $|\bar{\tau}| = 1$ is constant on all fault planes. The linear equation that we will solve is

$$\hat{\tau} = \sigma\hat{n} - [(\sigma\hat{n}) \cdot \hat{n}]\hat{n} = \hat{s}$$

$$\begin{bmatrix} n_1 - n_1^3 + n_1 n_3^2 & n_2 - 2n_2 n_1^2 & n_3 - 2n_3 n_1^2 & -n_1 n_2^2 + n_1 n_3^2 & -2n_1 n_2 n_3 \\ -n_2 n_1^2 + n_2 n_3^2 & n_1 - 2n_1 n_2^2 & -2n_1 n_2 n_3 & n_2 - n_2^3 + n_2 n_3^2 & n_3 - 2n_3 n_2^2 \\ -n_3 n_1^2 - n_3 + n_3^3 & -2n_1 n_2 n_3 & n_1 - 2n_1 n_3^2 & -n_2^2 n_3 - n_3 + n_3^3 & n_2 - 2n_2 n_3^2 \end{bmatrix} \begin{bmatrix} \sigma_{11} \\ \sigma_{12} \\ \sigma_{13} \\ \sigma_{22} \\ \sigma_{23} \end{bmatrix} = \begin{bmatrix} s_1 \\ s_2 \\ s_3 \end{bmatrix}$$

These normal equations are derived with the constraint that the isotropic stress is zero ($\sigma_{33} = -(\sigma_{11} + \sigma_{22})$) and can be rewritten in a compact form as

$$A^i \bar{\Sigma} = \hat{s}^i$$

where A^i is the sensitivity matrix, $\bar{\Sigma}$ is the vector of stress tensor elements and $\hat{s}^i$ are the elements of the slip direction vector. The sum is over the three slip directions for each event.

The normal equations have to be solved simultaneously for m = 55 earthquakes and $3m$ = 165 slip directions in order to obtain a single stress tensor that best represents all earthquakes. This is accomplished by stacking the normal equations for each event

$$\begin{bmatrix} A^1 \\ A^2 \\ A^3 \\ \cdot \\ \cdot \\ A^m \end{bmatrix} \vec{\Sigma} = \begin{bmatrix} \hat{s}^1 \\ \hat{s}^2 \\ \hat{s}^3 \\ \cdot \\ \cdot \\ \hat{s}^m \end{bmatrix}$$

The linear system can then be solved using linear least squares inversion to obtain the most likely stress tensor $\bar{\Sigma}$ that would explain the slip on all fault planes.

We estimate the deviatoric stress tensor for the Ninety East Ridge and Wharton Basin region by calculating the chi-square value and the residuals of the model slip values.

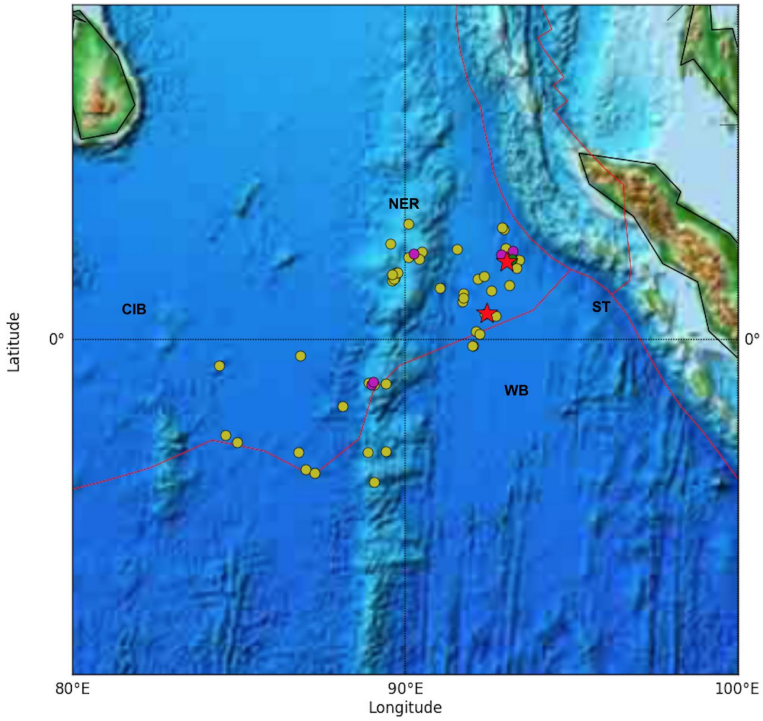

Fig 4. 55 selected earthquakes (M_W > 5.0) in the diffuse deformation zone that are included in the linear least squares regression. The M_W8.7 and M_W8.2 April 2012 earthquakes are plotted as red stars. Earthquakes are plotted according to magnitude (yellow: M_W5.0, magenta: M_W6.0, green: M_W7.0). Red lines represent tectonic boundaries. Abbreviations are as follows: NER, Ninetyeast Ridge; CIB, Central Indian Basin; WB, Wharton Basin; ST, Sunda Trench.

3.2 Results

We determined the deviatoric stress tensors and, by singular-value decomposition, principal stress directions for each of the earthquake nodal plane reported in the Global CMT catalog. The principal stresses S_1, S_2, S_3 in the stress tensor $\overline{\Sigma} = [S_1, S_2, S_3]$ are ordered from most compressional to most dilational in Table 1. The chi-square value for the stress tensor is $\chi_1^2 = 5.7$. Most of the residuals are randomly distributed between -0.2 and 0.2. A few outliers have more negative residuals.

The principal stresses represent a near-vertical S_2-axis and and near-horizontal S_1- and S_3-axes (Fig 5). They indicate predominantly strike-slip faulting along a fault plane oriented NW/SE or NE/SW. This agrees with the reported focal mechanisms of the earthquakes analyzed within this region, which are mostly strike-slip and thrust earthquakes oriented NW/SE. The most compressional axis (S_1) is oriented NW/SE and consistent with the P-axis directions of earthquakes in the Ninetyeast Ridge and Wharton Basin region (Fig 3).

Principal stresses	**Eigenvalue**	**Eigenvector**	**Azimuth (°)**	**Plunge (° from horizontal)**
S_1	-1.24	[-0.92,0.38,-0.14]	338	8
S_2	0.23	[-0.14,0.01,0.99]	177	82
S_3	1.0	[0.37,0.93,0.05]	68	3

Table 1. The eigenvalues, eigenvectors, azimuth and plunge of the principal stresses derived from the nodal planes of all 55 earthquakes in Fig 4.

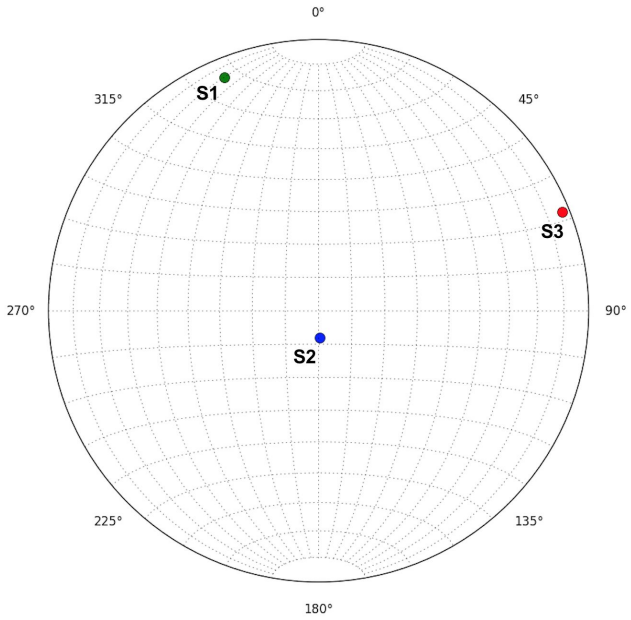

Fig 5. Principal stress orientations S1, S2, and S3 (see Table 1) on a stereonet determined from the 55 earthquakes in the southern Indian Ocean (Fig 4).

4. Waveform analysis to constrain earthquake focal depth

4.1 Comparison of synthetic and recorded seismograms

Recordings of the ground motion by seismographs provide information on the origin time, magnitude, depth and epicenter of an earthquake source. The time difference between the P wave and the S wave constrains the origin time and epicenter. Detail analysis of the waveform and dispersive pattern of the seismogram is necessary to constrain the depth of the earthquake. The Global Seismographic Network has more than 150 seismic recording stations located throughout the globe that monitor global seismic activity and share seismic data with the global seismological community.

The May 21, 2014 Bay of Bengal earthquake (M_W 6.1) was reported to have a source depth of 57.6 km (gCMT) and 47.23 km (NEIC). This intraplate earthquake is particularly interesting due to its deep source depth, large magnitude and isolated location away from other clusters of seismic events in the region (Fig. 6). By waveform analysis, we verify the reported depths using seismograms recorded at global network stations BJT (Baijiatuan, Beijing, China) and PALK (Pallekele, Sri Lanka). We generate synthetic displacement seismograms with varying focal depths using the method outlined by AxiSEM [Nissen-Meyer et al, 2014]. By visual inspection of the vertical and transverse component ground displacement recordings at BJT, we identify the synthetics that best matches the P-wave and S-wave arrivals of the recorded seismogram. Our focus is on the timing between P and the depth phases pP and sP and between SH and sSH which is strongly determined by source depth. By comparing the transverse displacement seismograms at PALK, we select the synthetic seismogram that best reproduces the dispersive nature of the surface wave.

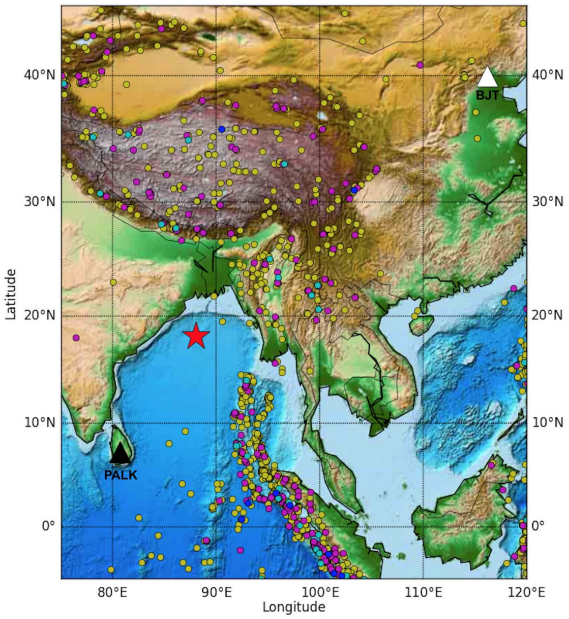

Fig 6. The May 2014 M_w6.1 Bay of Bengal earthquake (red star) is isolated from other intraplate seismic events. Waveform analysis is conducted on seismograms recorded at BJT (white triangle) and PALK (black triangle). Earthquakes occurring from Jan 1980 - Apr 2016 are plotted with colors according to magnitude (yellow: M_W5.0, magenta: M_W6.0, cyan: M_W7.0, blue: M_W8.0)

4.2 Results

We observe that both the depth phase arrival times and dispersive pattern comparisons confirm that the Bay of Bengal intraplate earthquake has a deep focal depth. The pP and sP arrivals that arrive about 15 s and 20 s after P and the sSH arrival that is recorded about 24 s after SH are best explained when the source depth is 50 km or 60 km (Fig 7A,B). Synthetics for

relatively large focal depth (> 30 km) also reproduce better the dispersive pattern of surface wave (Fig 8). At depth larger than 30 km, the S wave amplitude relative to the surface wave amplitude and the amplitude decay of the surface wave train is better for depths of 40, 50 and 60 km. At 30 km depth, the ratio of S-wave amplitude to surface wave amplitude is the same and at lower depths, the synthetics display the opposite ratio to the recorded seismogram. When filtered at frequency lower than 0.1 Hz (10 s period), the dispersive pattern at different source depths is less diagnostic because of the relatively high level of background noise in the ocean. This is evident from the low-amplitude, high-frequency waves prior to the first P-wave arrival in the recorded seismogram. The lowpass filter of 5 seconds and 10 seconds applied to the recorded seismogram removes the high frequency noise and helps us to better determine the phase arrivals and dispersive pattern. We also observe continued seismic recordings after 1400 seconds in the recorded seismogram (Fig 7C), which do not match the synthetic seismograms for any depth but this is primarily due to the poor 1-D background model used and the presence of wave scattering.

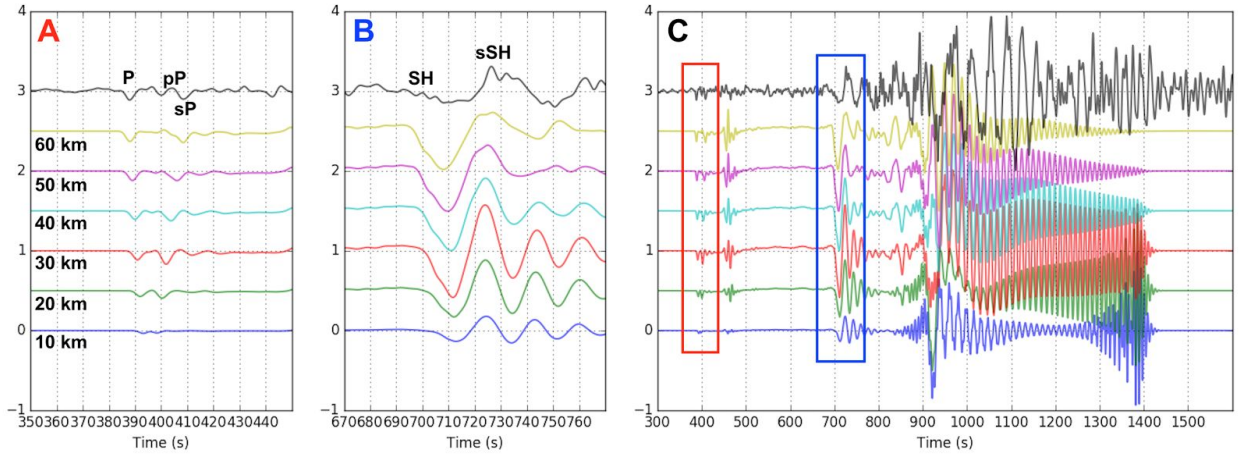

Fig 7. Vertical displacement plots of the May 2014 M_W6.1 Bay of Bengal earthquake recorded at BJT (Baijiatuan, China) station. (A) P, pP and sP wave arrivals and (B) SH and sSH wave arrivals of recorded and synthetic data filtered at 5 seconds. (C) Plot of recorded and synthetic data filtered at 5 seconds. Recorded data (top, black line) obtained from IRIS and synthetic data (multi-colored lines) generated using the AxiSEM method.

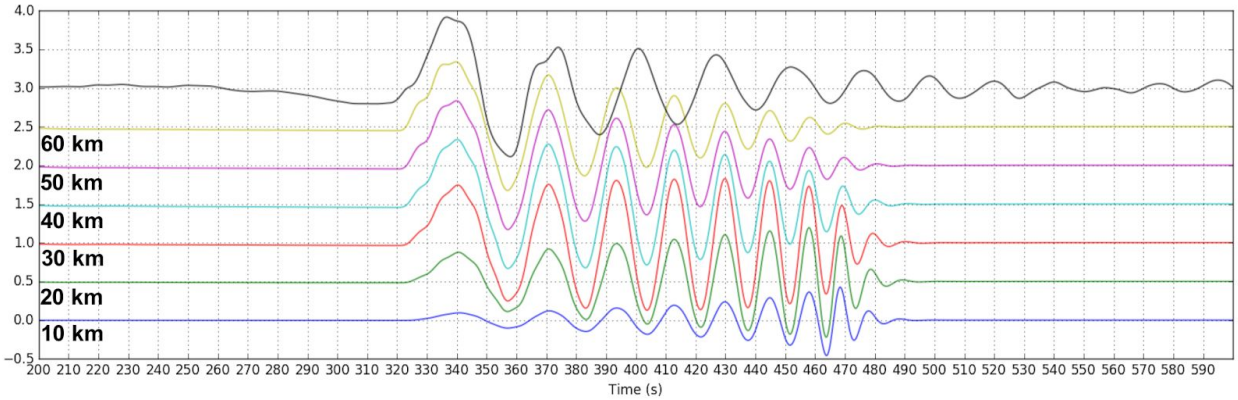

Fig 8. Transverse displacement plots of the May 2014 M_W6.1 Bay of Bengal earthquake recorded at PALK (Pallekele, Sri Lanka) for different focal depths filtered at 10 seconds. Recorded data (top, black line) obtained from IRIS and synthetic data (multi-colored lines) generated using the AxiSEM method.

Our results show that the event has a deep focal depth (40-60 km), consistent with faulting well below the crust, confirming the reported source depths for this event by gCMT and NEIC. However, we note that our focal depth estimates are fairly qualitative. Rigorous modeling with more accurate synthetics that account for wave propagation in a relatively thin crust should provide a more accurate estimates and well calibrated uncertainties.

5. Discussion

5.1 Diffuse Deformation Zone

The central tenet of plate tectonics in which plate interiors are rigid does not hold for the Indo-Australian plate. The high level of intraplate seismicity indicates that it there is internal deformation within the plate, or interactions between smaller subplates. The northwestern region of the Indo-Australian plate may be breaking up into three major component plates; the Indian Plate, Australian Plate and Capricorn Plate, along a broad diffuse deformation zone with undefined boundaries in the Indian Ocean (Fig 9) [Royer and Gordon, 1997; DeMets et al, 2009]. The deformation within the Indo-Australian Plate can be explained by the formation of two divergent zones neighboring the Central Indian Ridge and the Southeast Indian Ridge respectively and a larger convergent zone that spans the Central Indian Basin (CIB), Ninety East Ridge (NER) and Wharton Basin. The larger convergent zone is also interpreted as three diffuse convergent plate boundaries that meet at a diffuse triple junction between the Indian, Australian and Capricorn plates [Royer and Gordon, 1997]. Royer and Gordon (1997) proposed that a pole of rotation exists at 5°S, 74°E and that the Indian plate is diverging from the Capricorn Plate west of the pole and converging with the Australian Plate east of the pole. They also proposed

another pole of rotation at 25.8°S, 90°E where the Capricorn Plate is converging with the Australian plate NNE of the pole and the Capricorn Plate is diverging from the Australian plate SSW of the pole. The focal mechanisms of intraplate events show contrasting deformation styles according to the deformation pattern of each proposed plate boundary [Royer and Gordon, 1997]. In our earthquake magnitude plot (Fig. 3), we can observe the evidence of deformation within the Indo-Australian Plate from the numerous M_W>5.0 earthquakes scattered across the equatorial Indian Ocean. In the Ninetyeast Ridge and Wharton Basin region, 12 intraplate earthquakes with M_W>6.0 have occurred since 1980. This includes the largest strike-slip intraplate earthquakes ever recorded that occurred in April 2012 which was followed by several large aftershocks. Prior to this, two M_W6.2 events occurred close to the mainshock, one in 2006 and another in 2007. A M_W6.9 reverse-faulting earthquake occurred on the Ninety East Ridge (1.21°S,88.89°E) in January 1998 and another M_W6.4 strike-slip event occurred a year later at approximately the same location (1.25°S,88.98°E), in which both were striking NW-SE . In the Wharton Basin, M_W6.7 event occurred in October 1990 (2.20°S,92.29°E) while a M_W6.5 event occurred in June 2014 (10.02°S,91.06°E). Further south, a M_W7.9 event occurred in June 2000 (13.47°S,97.17°E)and more recently, a M_W7.8 strike-slip earthquake occurred in March 2016 (4.95°S,94.33°E). Adjacent to the Central Indian Ridge, a M_W7.7 event (6.89°S, 72.12°E) and M_W6.3 event (6.45°S,71.27°E) occurred a few days apart from each other in 1983. These uncharacteristically large intraplate earthquakes indicate that the equatorial region spanning the Central Indian Basin, Ninetyeast Ridge and Wharton Basin is under high stress and undergoing deformation.

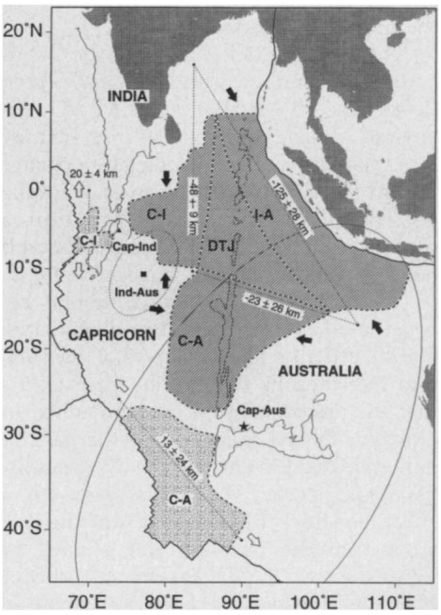

Fig 9. Map of the diffuse deformation zone in the Indo-Australian Plate. Black arrows indicate compression and white arrows indicate extension. Source: Royer and Gordon, 1997

The formation of a diffuse deformation zone in the Indo-Australian Plate is also supported by the pattern of compression indicated by the earthquake P-axis directions and the calculated regional stress fields. The cluster of intraplate earthquakes in the southeastern Indian Ocean have predominantly NW-SE P-axis directions, which indicate compressional deformation in this direction and high regional stress fields. We showed this in Section 3, where the most compressional principal stress for 55 earthquakes in this region is near horizontal and oriented NW-SE (Fig 5). This is consistent with the findings of Cloetingh and Wortel (1986) which showed that there is a concentration of compressive stress of the order of 3-5 kbar in the northern Ninetyeast Ridge area. They attributed the high compressive stress and the NW-SE P-axes orientation in the eastern Indian Ocean to the combination of the compressive forces from the India-Eurasia collision and the slab pull forces from the nearby Sunda Trench. The P-axis directions also agree with the current stress field of the eastern Indian Ocean [Muller et al, 2014] and is associated with the formation of plate boundaries within the diffuse deformation zone. The NW-SE P-axis directions adjacent to the Sunda Trench can be interpreted as the compressional boundary between the Indian and Australian plates. The NNW-SSE P-axis directions west of the Ninetyeast Ridge can be interpreted as the compressional boundary between the Indian and Capricorn plates while the WNW-ESE P-axis directions near the central Ninetyeast Ridge can be interpreted as the compressional boundary between the Capricorn and Australian plates [Royer and Gordon, 1997; DeMets et al, 2009]. The rotation of P-axis directions throughout the Indo-Australian Plate is attributed to the plate's geographic position relative to the surrounding plate boundaries and the variation of forces acting on the subducting slabs [Cloetingh and Wortel,1986].

5.2 May 2014 M_W6.1 Bay of Bengal intraplate earthquake

The large reported source depths of intraplate earthquakes (> 15 km) are unusual, since this indicates that the earthquakes are in the upper mantle. We expect mantle earthquakes to only occur in subduction zone tectonic settings and intraplate earthquakes to be limited to depths in the crust. We began our waveform analysis on the source depth of the May 2014 M_W6.1 Bay of Bengal earthquake with the assumption that there may be errors in the reported gCMT and NEIC source depths for this event, and possibly for other deep intraplate earthquakes. For oceanic earthquakes, the transfer of seismic energy from the oceanic crust to the ocean water creates noise in the seismogram which makes it difficult to discern the P-wave arrival. Therefore, erroneous determination of the first P-wave arrival may result in the large reported source depths for these earthquakes.

Our analysis does not fully capture the complexities of the recorded data. The synthetic data is generated using PREM (Preliminary Earth Reference Model), a one-dimensional model for the structure of the Earth [Dziewonski and Anderson, 1981]. It does not account for the

thinner oceanic crust where the source is generated and also the thicker crust in the Himalayan Front. In order to conduct waveform analysis on this earthquake, we selected the seismic stations based on angular distance from the earthquake epicenter. For the phase arrival analysis, we chose to analyze data from the BJT station due to its relatively long distance from the source. The BJT station is located 32.6° away from the epicenter of the earthquake and is therefore less sensitive to the thickness of the crust. Thus, we are able to avoid the complexities of waves travelling through the thick Tibetan crust. For the dispersive pattern analysis, we chose to analyze data from the PALK station, which is located 13.06 degrees southwest of the epicenter of the earthquake. The shorter distance and the mostly oceanic path from the source to PALK allows us to observe the dispersive pattern clearly. However, since we are using PREM Earth model with a 24 km thick crust in our analysis, our results cannot be verified with certainty.

Researchers have taken various approaches to study this earthquake including waveform analysis, structural mapping of the Bengal Basin and analysis of its seismic intensity. It is generally agreed that seismicity in the Bay of Bengal is attributed to compressional forces at the Himalayan Front. Mallick and Rajendran [2015] and Rai et al [2015] conducted waveform analyses on the earthquake and concluded that the earthquake occurred along a NW-SE oriented fault with a near vertical motion. Both also found a deep focal depth for the earthquake, where Mallick and Rajendran [2015] inferred a depth of 54 km from age-focal depth relationships for global oceanic intraplate earthquakes while Rai et al inferred a depth of 61 km, below the suggested lower boundary of the crust. Rao et al [2015] analyzed focal mechanism solutions for earthquakes that occurred along the east coast of India and the Bay of Bengal and also mapped structural and tectonic features in the Bengal Basin. The authors also conclude that the earthquake occurred along a NW-SE oriented fault with a right-lateral sense of motion. Rai et al [2015] and Rao et al [2015] suggested that the earthquake was caused by the reactivation of paleo-faults and fracture zones in the Bay of Bengal while Mallick and Rajendran [2015] suggested the earthquake is associated the 85°E ridge and reactivation of hotspot trails. The deep focal depth of the earthquake is attributed to the high mechanical strength of the upper part of the oceanic lithosphere [Rai et al, 2015]. From analysis of seismic intensity, Martin and Hough [2015] reported a high stress drop for the earthquake and they attributed this to its deep focal depth.

We conclude that the Indo-Australian Plate is undergoing internal deformation which explains the high occurrence of M_W>5.0 intraplate earthquakes. Our analysis of the P-axes directions of intraplate earthquakes indicate that patterns of compression related to the dynamic forces acting along different plate boundaries and the possible formation of a diffuse deformation zone in the southern Indian Ocean. The principal stress directions that we found for 55 intraplate earthquakes in the southern Indian Ocean also agree with the general stress directions of earthquakes in the region. Using waveform analysis, we confirm the focal depth of the May 21,

2014 Bay of Bengal earthquake to be between 40-60 km, as reported by gCMT and NEIC. However, the causes for the occurrence of this exceptionally deep earthquake and other deep intraplate earthquakes in the Indo-Australian Plate is still unclear and would be an interesting topic for further research.

6. Acknowledgements

I would like to express my sincere gratitude to my research advisor, Professor Jeroen Ritsema, for his continuous support and guidance throughout the duration of this research project. I am thankful for the opportunity that he gave me to be involved in an independent undergraduate research project and for the immense knowledge that he has imparted to me as part of this process. My sincere thanks also goes to Sam Haugland, a graduate student in my department, who has assisted me in learning the programming aspects of my research project. Without their support and motivation, I would not be able to complete this thesis.

7. References

Andrade, V., Rajendran, K., 2014. The April 2012 Indian Ocean earthquakes: Seismotectonic context and implications for their mechanisms. *Tectonophysics* 617 (2014).

Cande, S. C., Kent, D. V., 1995. Revised calibration of the geomagnetic polarity timescale for the Late Cretaceous and Cenozoic, *J. Geophys. Res.*, 100(B4), 6093–6095.

Cloetingh, S., Wortel, R., 1986. Stress in the Indo-Australian plate. *Tectonophysics* 132, 49-67.

DeMets, C., Gordon, R.G., Argus, D.F., 2009. Geologically current plate motions. *Geophys. J. Int.* 181, 1-80.

Dziewonski A.M., Anderson, D.L., 1981. Preliminary reference Earth model. *Physics of the Earth and Planetary Interiors* 25, 297-356.

Dziewonski, A. M., Chou, T.A., Woodhouse, J.H., 1981. Determination of earthquake source parameters from waveform data for studies of global and regional seismicity. *J. Geophys. Res.* 86, 2825-2852.

Ekström, G., Nettles, M., Dziewonski, A.M., 2012. The global CMT project 2004-2010: Centroid-moment tensors for 13,017 earthquakes. *Phys. Earth Planet. Inter.*, 200-201, 1-9.

Krishna, K.S., Gopala Rao, D., Ramana, M.V., Subrahmanyam, V., Sarma, K.V.L.N.S., Pilipenko, A.I.,

Scherbakov, V.S., Radhakrishna Murthy, I.V., 1995. Tectonic model for the evolution of oceanic crust in the northeastern Indian Ocean from the Late Cretaceous to early Tertiary. *J. Geophys. Res.* 100, 20,011-20,024.

Mallick, R., Rajendra, K., 2015. The 2014 Mw6.1 Bay of Bengal, Indian Ocean, Earthquake: A possible association with the 85° Ridge. *Bulletin of the Seismological Society of America* 106, 408-417.

Martin, S. S., Hough, S.E., 2015. The 21 May 2014 Mw 5.9 Bay of Bengal earthquake: Macroseismic data suggest a high-stress-drop event, *Seismological Research Letters* 86, 369–377.

Michael, A.J., 1984. Determination of stress from slip data: Faults and folds. *Journal of Geophysical Research* 89. 11,517-11,526.

Muller, R.D, Yatheesh, V., Shuhail, M., 2015. The tectonic stress field evolution of India since the Oligocene. *Gondwana Research* 28, 612-624.

Nissan-Meyer, T., van Driel, M., Stahler, S.C., Hosseini, K., Hempel, S., Auer, L., Colombi, A., Fournier, A., 2014. AxiSEM: broadband 3-D seismic wavefields in axisymmetric media. *Solid Earth* 5, 425-445.

Plate Motion Calculator. *UNAVCO.org*. Web.
<http://www.unavco.org/software/geodetic-utilities/plate-motion-calculator/plate-motion-calculator.html>

Rai, A.K., Tripathy, S., Sahu, S.C., 2015. The May 21st, 2014 Bay of Bengal earthquake: implications for intraplate stress regime. *Current Science* 108, 1706-1712.

Rao G.S., Radhakrishna, M., Murthy, K.S.R., 2015. A seismotectonic study of the 21 May 2014 Bay of Bengal intraplate earthquake: evidence of onshore-offshore tectonic linkage and fracture zone reactivation in the northern Bay of Bengal. *Nat Hazards* 78, 895-913.

Royer, J-Y., Gordon, R.G., 1997. The motion and boundary between the Capricorn and Australian Plates. *Science* 277, 1268-1274.

Satriano C., Kiraly, E., Bernard, P., Vilotte, J-P., 2012. The 2012 Mw 8.6 Sumatra earthquake: Evidence of westward sequential seismic ruptures associated to the reactivation of a N-S ocean fabric. *Geophysical Research Letters* 39, L15302.

Whittaker, J.M., Muller, R.D., Sdrolias, M., Heine, C., 2007. Sunda-Java trench kinematics, slab window formation and overriding plate deformation since the Cretaceous. *Earth and Planetary Science Letters* 255, 445-457.

Yue, H., Lay, T., Koper, K.D., 2012. En echelon and orthogonal fault ruptures of the 11 April 2012 great intraplate earthquakes. *Nature* 490, 245-249.